Estimating of Fraction of Weakly Deformable Erythrocytes in a Blood Sample Based on the Method of Laser Ektacytometry and a Database of Simulated Diffraction Patterns

Vladislav D. Ustinov, Evgeniy G. Tsybrov*, and Sergey Y. Nikitin
M. V. Lomonosov Moscow State University, GSP-1 Leninskie Gory, Moscow 119991, Russia

***e-mail:** tsybrovevgeniy@yandex.ru

Abstract. The problem of measuring the fraction of weakly deformable erythrocytes in a blood sample by the laser diffractometry in a shear flow (ektacytometry) is considered. The algorithm for measuring this parameter is proposed, based on a comparison of experimentally observed diffraction patterns with ones calculated in the bimodal ensemble approximation, when only two types of erythrocytes are present in a blood sample – normal (deformable) and rigid (non-deformable) erythrocytes. The accuracy of the algorithm was estimated by the method of numerical experiment and the area of its applicability was determined. © 2023 Journal of Biomedical Photonics & Engineering.

Keywords: erythrocyte deformability; laser ektacytometry; data processing algorithms.

Paper #7216 received 21 Feb 2023; revised manuscript received 15 Jun 2023; accepted for publication 16 Jun 2023; published online 22 Jul 2023. doi: 10.18287/JBPE23.09.030303.

1 Introduction

One of the main rheological characteristics of blood is the deformability of erythrocytes, which is defined as a measure of the ability of blood cells to change their shape under the action of external forces [1–4].

Rapid measurements of the deformability characteristics of erythrocytes are possible based on the method of laser diffractometry in shear flow (ektacytometry) [5–9]. This method is based on the observation and analysis of diffraction patterns arising at the scattering of a laser beam by a suspension of erythrocytes in a given field of shear stresses. Currently, there are laser erythrocyte ektacytometers – Lorrca (Netherlands) and RheoScan (Republic of Korea) [10], which can be used to measure the average deformability of the erythrocytes. At the same time, the problem of measuring the distribution of erythrocytes in deformability [11–14] is great of significance, in particular, the problem of measuring the fraction of weakly deformable erythrocytes in a blood sample [15–19]. In this paper, we propose an algorithm for measuring the fraction of weakly deformable erythrocytes based on comparing the experimentally observed diffraction pattern with the pattern calculated in the bimodal ensemble approximation, when only two types of erythrocytes are present in a blood sample: normal (deformable) and rigid (non-deformable) erythrocytes.

2 Laser Ektacytometry of Erythrocytes

In a rotary ektacytometer, a diluted suspension of erythrocytes is poured into a narrow gap between the walls of two transparent coaxial cups, one of which is stationary and the other can be rotated with a given angular velocity. The rotation of the outer cup leads to arising a shear stress in the suspension, which elongate the erythrocytes in the direction of the shear flow. The suspension is illuminated with a laser beam, the image of the pattern of light scatter by erythrocytes is registrated and analyzed using a special algorithm. Examples of the diffraction patterns obtained for a normal blood sample are shown at the Fig. 1. At low shear stress, the diffraction pattern has circular symmetry (Fig. 1a). At high shear stress, the pattern is elongated (Fig. 1b), demonstrating the deformation of erythrocytes by viscous friction forces.

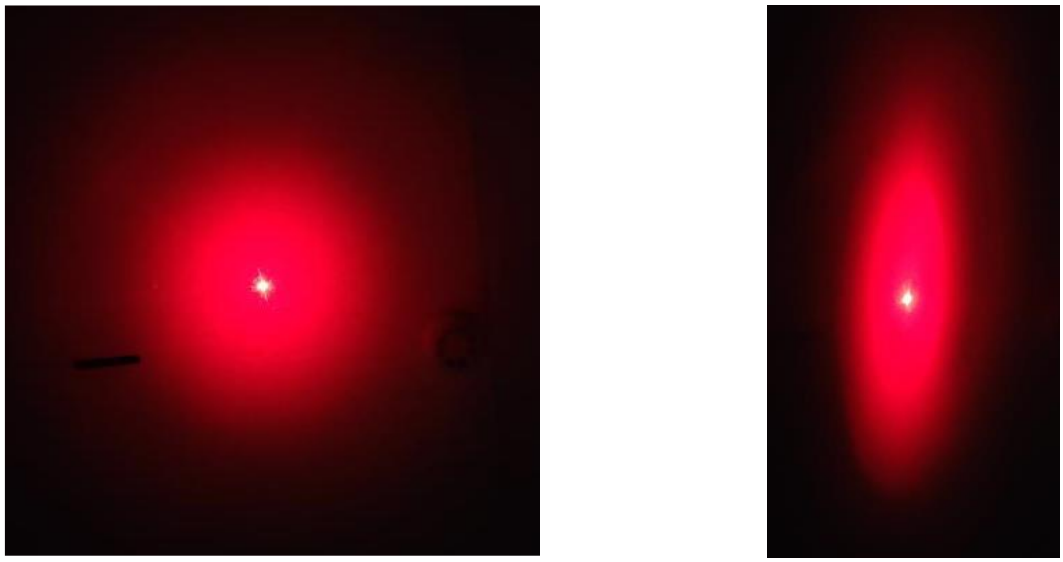

(a) (b)

Fig. 1 Diffraction patterns obtained by the laser erythrocyte ektacytometer for a normal blood sample at low (a) and high (b) shear stresses. The blood sample was taken from a healthy man at the age of 25 years.

3 Model of a Bimodal Ensemble of Erythrocytes

The simplest model of a blood sample containing cells with reduced deformability is the model of a bimodal ensemble of erythrocytes, which assumes the presence of only two types of cells in the blood - normal (deformable) erythrocytes and rigid (non-deformable) erythrocytes. Erythrocytes in shear flow acquire a shape close to ellipsoidal [11, 12]. For simplicity, we will model erythrocytes with flat elliptical disks. This makes it possible to describe the scattering of a laser beam by erythrocytes in an analytical form, and on this basis to build algorithms for processing laser ektacytometry data. An elliptical disk is characterized by the dimensions of its semi-axes a and b and the aspect ratio $s = a/b$. In the bimodal ensemble, there are two types of erythrocytes with semiaxes a_1, b_1 and a_2, b_2 and aspect ratios $s_1 = a_1/b_1$ and $s_2 = a_2/b_2$. Let us denote the fraction of the first type erythrocytes in a blood sample as p. Considering erythrocytes of the first type as rigid (non-deformable) cells, we set $s_1 = 1$. Erythrocytes of the second type are considered normal, for them $s_2 > 1$, and this value depends on the shear stress in the ektacytometer (or elongation of the cell at certain shear stress). In our calculations, we will change the parameter s_2 at a certain range, thus modeling ensembles of erythrocytes with differences in the degree of heterogeneity of the bimodal ensemble.

4 Diffraction Pattern

The diffraction pattern of laser beam scattering by an inhomogeneous ensemble of erythrocytes was calculated in Ref. [20, 21]. For a bimodal ensemble, it is described by the following Eq. [22]:

$$\tilde{I}(x,y) = \frac{p\cdot(a_1b_1)^2 G\left(\frac{k}{z}\sqrt{a_1^2x^2+b_1^2y^2}\right)+(1-p)\cdot(a_2b_2)^2 G\left(\frac{k}{z}\sqrt{a_2^2x^2+b_2^2y^2}\right)}{p\cdot(a_1b_1)^2+(1-p)\cdot(a_2b_2)^2}.$$

Here $\tilde{I}$ is the light intensity normalized to the intensity of the central maximum of the diffraction pattern, x, y are the Cartesian coordinates of a point on the observation screen, z is the distance from the measuring volume to the observation screen, $k = 2\pi/\lambda$ is the wavenumber, λ is the wavelength of the laser beam, p is the fraction of weakly deformable erythrocytes in a blood sample. The function $G(x)$ is defined by the following Eq.:

$$G(\mathrm{x}) = [2J_1(x)/x]^2,$$

where $J_1(x)$ is the first order Bessel function. The remaining parameters are expressed by the Eqs.:

$$a_1 = a_0 \cdot (1 + \varepsilon_1), \qquad b_1 = b_0 \cdot (1 - \varepsilon_1),$$

$$a_2 = a_0 \cdot (1 + \varepsilon_2), \qquad b_2 = b_0 \cdot (1 - \varepsilon_2),$$

$$M = (s_1 - s_2) \cdot \left(p - \frac{1}{2}\right),$$

$$s = M + \sqrt{M^2 + s_1 s_2},$$

$$\varepsilon_1 = \frac{s_1 - s}{s_1 + s}, \qquad \varepsilon_2 = \frac{s_2 - s}{s_2 + s},$$

$$b_0 = a_0/s.$$

Here a_0 and b_0 are the average sizes of the semi-axes of the elliptical disk.

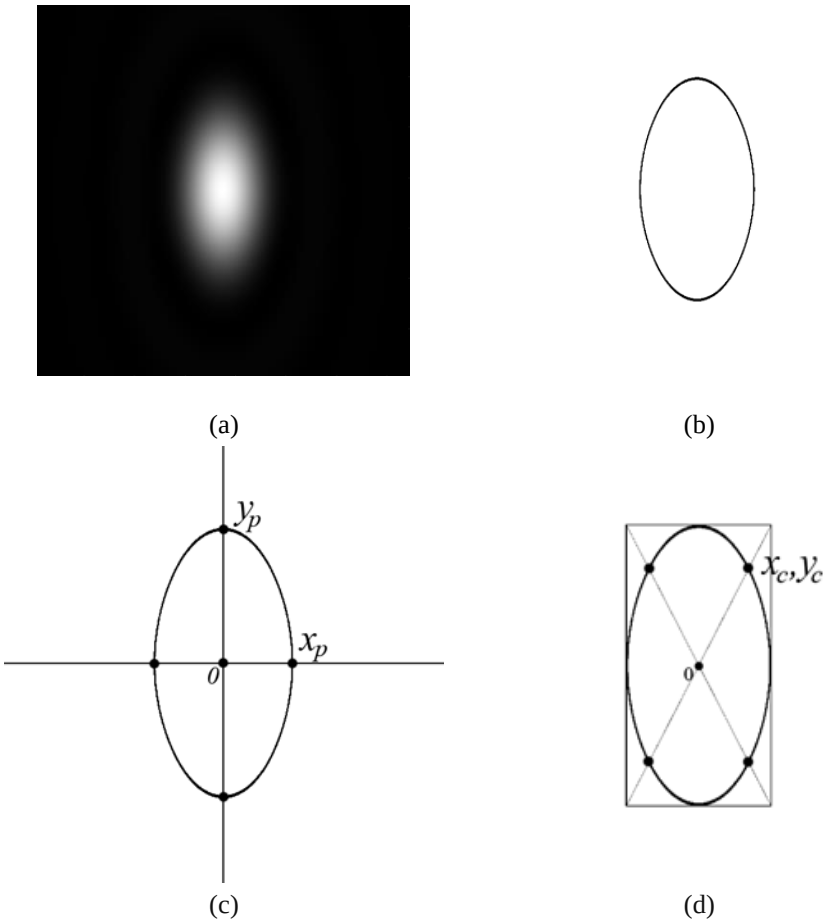

Fig. 2 Example of a diffraction pattern (a), isointensity line (b), its polar (c) and characteristic points (d). The diffraction pattern was constructed numerically for a bimodal ensemble of erythrocytes with parameters $s_1 = 1$, $s_2 = 2.02$, and $p = 0.062$. The isointensity line corresponds to the level $\tilde{I} = 0.05$. The parameters of the polar and characteristic points of this line are $D_e = 1.945$, $Q_e = 0.984$.

5 Iso-Intensity Line, Polar, and Characteristic Points

The analysis of the diffraction pattern is carried out on the basis of the concept of the isointensity line. This is the name of the set of points on the observation screen, the light intensity in which has a certain value $\tilde{I} = const$. The isointensity line equation has the form

$$\frac{p\cdot(a_1b_1)^2 G\left(\frac{k}{z}\sqrt{a_1^2x^2+b_1^2y^2}\right)+(1-p)\cdot(a_2b_2)^2 G\left(\frac{k}{z}\sqrt{a_2^2x^2+b_2^2y^2}\right)}{p\cdot(a_1b_1)^2+(1-p)\cdot(a_2b_2)^2} = \tilde{I}.$$

This Eq. implicitly defines the function $x = x(y)$ or $y = y(x)$, which describes the shape of the iso-intensity line. The form of this function can be found numerically. Let us introduce the concepts of polar and characteristic points of the isointensity line. Points of intersection of the iso-intensity line with the Cartesian coordinate axes (symmetry axes of the iso-intensity line) are called polar. The characteristic points are the points of intersection of the iso-intensity line with the diagonals of the rectangle enclosing this line. An example of a diffraction pattern, an isointensity line, as well as its polar and characteristic points (numerical simulation data) are shown in Fig. 2.

Due to the symmetry of the iso-intensity line, it suffices to consider the upper and right polar points and one characteristic point. Let us denote the coordinates of the upper polar point $x = 0, y = y_p$, the coordinates of the right polar point $x = x_p, y = 0$, the coordinates of the characteristic point $x = x_c, y = y_c$. Let us introduce the parameters [23]:

$$D = \frac{y_p}{x_p},$$

$$Q = \frac{1}{\sqrt{2}}\left(\frac{x_c}{x_p} + \frac{y_c}{y_p}\right).$$

As can be seen from Fig. 2,

$$y_c = x_c \frac{y_p}{x_p}.$$

Hence

$$y_c = x_c D,$$

$$Q = \sqrt{2}\frac{x_c}{x_p}.$$

Parameters D and Q can be measured experimentally using a laser erythrocyte ektacytometer or calculated theoretically based on a particular model. Our further task is to find the relationship between these parameters and the characteristics of the bimodal ensemble of erythrocytes p and s_2, and on this basis to develop an algorithm for measuring the fraction of weakly deformable erythrocytes p in a blood sample.

6 Database of Simulated Diffraction Patterns Building

The database of simulated diffraction patterns is a set of solutions of the direct scattering problem, when the known parameters of the ensemble of erythrocytes are used to find the characteristics of the diffraction pattern that occurs when a laser beam is scattered by blood samples with different initial distribution parameters. When constructing the database, we will consider the parameters of the erythrocyte ensemble s_1, s_2, p as well as the level of light intensity $\tilde{I}$ on the iso-intensity line chosen for measurements, to be known. We will calculate the geometric parameters of the iso-intensity line - the parameter of the polar points D and the parameter of the characteristic point Q. For a given value of the parameter $\tilde{I}$, the database is a function set of two variables $D = D(p, s_2)$ and $Q = Q(p, s_2)$ specified in table form. Calculations are made as follows.

Let us introduce the normalized coordinates of a point on the screen for observing the diffraction pattern U and V, defining them by the Eqs.:

$$x = \frac{z}{ka_0}U,$$

$$y = \frac{z}{kb_0}V.$$

In these coordinates, the isointensity line equation takes the form [24]

$$\frac{pe_1G\left(\sqrt{e_{1u}^2U^2+e_{1v}^2V^2}\right)+(1-p)e_2G\left(\sqrt{e_{2u}^2U^2+e_{2v}^2V^2}\right)}{pe_1+(1-p)e_2} = \tilde{I},$$

where

$$e_1 = (1-\varepsilon_1^2)^2, \qquad e_2 = (1-\varepsilon_2^2)^2,$$

$$e_{1u} = 1+\varepsilon_1, \qquad e_{2u} = 1+\varepsilon_2,$$

$$e_{1v} = 1-\varepsilon_1, \qquad e_{2v} = 1-\varepsilon_2.$$

Normalized coordinates of the upper polar point $U = 0$, $V = V_p$, right polar point $U = U_p$, $V = 0$, characteristic point $U = U_c$, $V = V_c$. Polar and characteristic point parameters

$$D = s\frac{V_p}{U_p},$$

$$Q = \sqrt{2}\frac{U_c}{U_p}.$$

The Eqs. for the coordinates U_p, V_p, U_c of the polar and characteristic points have the form

$$\frac{pe_1G(e_{1u}U_p)+(1-p)e_2G(e_{2u}U_p)}{pe_1+(1-p)e_2} = \tilde{I},$$

$$\frac{pe_1G(e_{1v}V_p)+(1-p)e_2G(e_{2v}V_p)}{pe_1+(1-p)e_2} = \tilde{I},$$

$$\frac{pe_1G\left(\frac{U_c}{U_p}\sqrt{e_{1u}^2U_p^2+e_{1v}^2V_p^2}\right)+(1-p)e_2G\left(\frac{U_c}{U_p}\sqrt{e_{2u}^2U_p^2+e_{2v}^2V_p^2}\right)}{pe_1+(1-p)e_2} = \tilde{I}.$$

By setting the parameters of the bimodal ensemble of erythrocytes s_1, s_2, p as well as the level of light intensity on the isointensity line $\tilde{I}$, these Eqs. can be used to calculate the parameters of the diffraction pattern D and Q of interest to us. In all cases, we assumed $s_1 = 1$, which corresponds to the presence in the ensemble erythrocytes are rigid (non-deformable) cells. As an example, Tables 1 and 2 show the fragment of the database obtained for $\tilde{I} = 0.05$. All numbers in Tables 1 and 2 are given with an accuracy of three decimal places.

Table 1 Parameter D values.

		p		
		0	**0.05**	**0.1**
s_2	**1.95**	1.948	1.891	1.831
	2.00	2.000	1.940	1.877
	2.05	2.049	1.987	1.919

Table 2 Parameter Q values.

		p		
		0	**0.05**	**0.1**
s_2	**1.95**	1.000	0.988	0.975
	2.00	1.000	0.987	0.974
	2.05	1.000	0.987	0.972

The volume of the database is indicated in Section 9.

7 Measurement Algorithm

The task of ektacytometry is to find the characteristics of the ensemble of erythrocytes p and s_2 from the known parameters of the diffraction pattern D_e and Q_e. To do this, we need to solve the Eqs.:

$$D(p, s_2) = D_e,$$

$$Q(p, s_2) = Q_e.$$

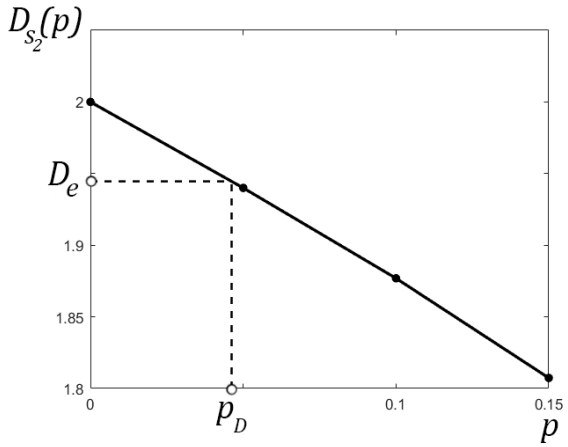

(a)

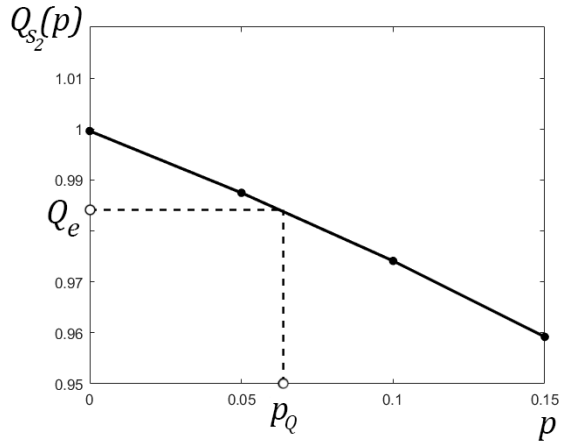

(b)

Fig. 3 Graphs of the functions $D_{s2}(p)$ (a) and $Q_{s2}(p)$ (b) constructed for $s_2 = 2$ and и $\tilde{I} = 0.05$.

where the functions $D(p, s_2)$ and $Q(p, s_2)$ are defined as database tables. The problem is solved in the following way. With a fixed value of the parameter s_2, the values D and Q become functions of one variable, the parameter p. Let us denote these functions as $D_{s2}(p)$ and $Q_{s2}(p)$. An analysis of the tables shows that both of these functions are monotonically decreasing. They can be approximated with good accuracy by continuous piecewise linear functions. This allows each number s_2 from the database to be associated with a number p_D such that $D_{s2}(p_D) = D_e$ and a number p_Q such that $Q_{s2}(p_Q) = Q_e$. As an example, Fig. 3 shows the graphs of the functions $D_{s2}(p)$ and $Q_{s2}(p)$ constructed for $s_2 = 2$ and $\tilde{I} = 0.05$.

Repeating such calculations for different values of the number s_2, we obtain the functions $p_D(s_2)$ and $p_Q(s_2)$, given in the form of tables. In the region of parameter change of interest to us, one of these functions is monotonically increasing, and the second is monotonically decreasing. These functions can also be approximated with good accuracy by continuous piecewise linear functions. This makes it possible to find the number s_2, at which $p_D(s_2) = p_Q(s_2)$, and determine the corresponding value of the number p such that $p = p_D(s_2) = p_Q(s_2)$. As an example, Fig. 4 shows the graphs of the functions $p_Q(s_2)$ and $p_D(s_2)$ constructed for $\tilde{I} = 0.05$, $D_e = 1.945$ and $Q_e = 0.984$.

Mathematically, these procedures are expressed by the following Eqs.:

$$p_D(s_2) = \frac{(D_2 - D_e)p_{1D} + (D_e - D_1)p_{2D}}{D_2 - D_1}, \quad (1)$$

$$p_Q(s_2) = \frac{(Q_2 - Q_e)p_{1Q} + (Q_e - Q_1)p_{2Q}}{Q_2 - Q_1}, \quad (2)$$

$$p = \frac{p_Q(s_{22})p_D(s_{21}) - p_D(s_{22})p_Q(s_{21})}{p_Q(s_{22}) - p_Q(s_{21}) - p_D(s_{22}) + p_D(s_{21})}, \quad (3)$$

$$s_2 = \frac{[p_Q(s_{22}) - p_D(s_{22})]s_{21} + [p_D(s_{21}) - p_Q(s_{21})]s_{22}}{p_Q(s_{22}) - p_Q(s_{21}) - p_D(s_{22}) + p_D(s_{21})}. \quad (4)$$

Here numbers D_1, D_2 are neighboring numbers from row s_2 of the table of parameter D values such that

$$D_1 \le D_e \le D_2.$$

The numbers p_{1D}, p_{2D} are the values of the number p such that

$$D_{s2}(p_{1D}) = D_1,$$

$$D_{s2}(p_{2D}) = D_2.$$

The numbers Q_1, Q_2 are neighboring numbers from the row s_2 of the table of Q parameter values such that

$$Q_1 \le Q_e \le Q_2.$$

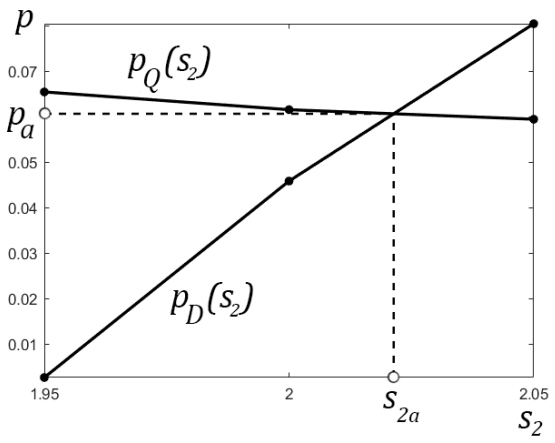

Fig. 4 Graphs of functions $p_D(s_2)$ and $p_Q(s_2)$ constructed for $\tilde{I} = 0.05$, $D_e = 1.945$, and $Q_e = 0.984$.

The numbers p_{1Q}, p_{2Q} are the values of the number p p such that

$$Q_{s2}(p_{1Q}) = Q_1,$$

$$Q_{s2}(p_{2Q}) = Q_2.$$

The numbers s_{21}, s_{22} are neighboring values of the number s_2 from the database such that the values $p_D(s_{21}) - p_Q(s_{21})$ and $p_D(s_{22}) - p_Q(s_{22})$ have different signs.

8 Verification of the Algorithm by Numerical Experiment

Let the bimodal ensemble of erythrocytes be characterized by the parameters

$$s_1 = 1, \qquad s_2 = 2.02, \qquad p = 0.062.$$

The pattern of laser beam scattering by such an ensemble is shown in Fig. 2a. Let us choose the iso-intensity line of the diffraction pattern at the level of relative light intensity

$$\tilde{I} = 0.05.$$

This line is shown in Fig. 2b, its polar and characteristic points are shown in Figs. 2c and 2d. The parameters of the polar and characteristic points of this line have the following numerical values

$$D_e = 1.945, \qquad Q_e = 0.984.$$

To solve the inverse scattering problem, we use the data given in Tables 1 and 2. From Table 1 for

$$s_2 = 1.95$$

using conditions

$$D_1 \le D_e \le D_2$$

we find

$$D_1 = 1.891, \qquad D_2 = 1.948,$$

and the values of the parameter p corresponding to these numbers

$$p_{1D} = 0.05, \qquad p_{2D} = 0.$$

Further, according to Eq. (1), we obtain

$$p_D(s_2 = 1.95) = 0.0026.$$

The procedure for finding this number is illustrated in Fig. 3a. Acting similarly, we find several private values of the functions $p_D(s_2)$ and $p_Q(s_2)$:

$$p_D(s_2 = 1.95) = 0.0026, \quad p_Q(s_2 = 1.95) = 0.0654,$$

$$p_D(s_2 = 2.00) = 0.0458, \quad p_Q(s_2 = 2.00) = 0.0615,$$

$$p_D(s_2 = 2.05) = 0.0804, \quad p_Q(s_2 = 2.05) = 0.0594.$$

It follows that the difference $p_D(s_2) - p_Q(s_2)$ changes sign when

$$s_{21} \le s_2 \le s_{22},$$

where

$$s_{21} = 2.00, \qquad s_{22} = 2.05.$$

The partial values of the functions $p_D(s_2)$ and $p_Q(s_2)$ at these points are found by Eqs. (1), (2) and we obtain

$$p_D(s_{21}) = 0.0458, \qquad p_D(s_{22}) = 0.0804,$$

$$p_Q(s_{21}) = 0.0615, \qquad p_Q(s_{22}) = 0.0594.$$

Finally, using Eqs. (3), (4), we calculate the required parameters of the ensemble of erythrocytes

$$p_a = 0.061, \qquad s_{2a} = 2.02.$$

Comparing these numbers with the initially given (true) values of these parameters

$$p = 0.062, \qquad s_2 = 2.02,$$

we conclude that in this case the parameter s_2 is determined exactly, and the parameter p is determined with an error of less than 2%. Thus, for typical experimental conditions, the accuracy of the database-based algorithm turns out to be very high.

9 Results

Calculations of parameters D and Q of diffraction patterns were performed for the following values of parameters of bimodal ensembles of erythrocytes:

$$s_1 = 1,$$

$1.9 \le s_2 \le 3$ with step $\Delta s_2 = 0.05$ (total 23 numbers s_2),

$0 \le p \le 0.5$ with step $\Delta p = 0.05$ (total 11 p numbers),

and levels of relative light intensity on the iso-intensity line

$$\tilde{I} = 0.03;\ 0.05;\ 0.07;\ 0.09;\ 0.15;\ 0.25;\ 0.4;\ 0.5.$$

In total, 1928 D numbers and 1928 Q numbers were found. These numbers form a database, i.e. a set of solutions to the direct problem of diffractometry.

The database algorithm check was made for the following parameter values:

$$s_1 = 1,$$

$$s_2 = 2.02;\ \ 2.92,$$

$$p = 0.0075;\ 0.015;\ 0.031;\ 0.062;\ 0.125;\ 0.25,$$

$$\tilde{I} = 0.03;\ 0.05;\ 0.07;\ 0.09;\ 0.15;\ 0.25;\ 0.4.$$

The accuracy of the algorithm and the area of its applicability are characterized by the data presented in Tables 3 and 4. These tables indicate the error in determining the fraction of weakly deformable erythrocytes in the bimodal ensemble, found by numerical simulation of diffraction patterns and their analysis using the database algorithm.

Table 3 Error in determining the fraction of weakly deformable erythrocytes in a bimodal ensemble (in percent) based on the database algorithm – numerical experiment (s_1 = 1, s_2 = 2.02).

		p				
		0.015	**0.031**	**0.062**	**0.125**	**0.25**
$\tilde{I}$	**0.03**	6.6	5.5	1.8	0.7	1.0
	0.05	0.7	9.1	1.4	0.5	0.8
	0.07	1.3	4.3	4.5	1.5	0.0
	0.09	13.7	2.6	1.5	4.0	2.4
	0.15	10.0	39.5	8.2	0.7	0.9

Table 4 Error in determining the fraction of weakly deformable erythrocytes in a bimodal ensemble (in percent) based on the database algorithm – numerical experiment (s_1 = 1, s_2 = 2.92).

		p				
		0.015	**0.031**	**0.062**	**0.125**	**0.25**
$\tilde{I}$	**0.03**	17.3	5.0	2.2	12.2	2.2
	0.05	0.6	8.7	1.0	1.0	0.1
	0.07	10.8	4.5	3.2	1.4	0.2
	0.09	23.3	7.6	1.6	0.5	0.4
	0.15	36.3	7.1	6.2	1.9	0.2

It can be seen from Tables 3 and 4 that the error in measuring the number p does not exceed 10% in the region of parameter values

$$0.03 \le \tilde{I} \le 0.09$$

and

$$0.03 \le p \le 0.25$$

which corresponds to the spread of erythrocytes in deformability

$$0.087 \le \mu' \le 0.23 \qquad \text{for } s_2 = 3,$$

$$0.058 \le \mu' \le 0.15 \qquad \text{for } s_2 = 2.$$

Here the parameter μ' is defined by the Eq.:

$$\mu' = \sqrt{p\varepsilon_1^2 + (1-p)\varepsilon_2^2}$$

and has the meaning of the standard deviation of the deformability of erythrocytes in a bimodal ensemble from its average value. For the levels of relative light intensity $\tilde{I} = 0.25$ and $\tilde{I} = 0.40$, the measurement error of parameter p using the database algorithm, as a rule, exceeds 10%. As for the measurement error of parameter s_2, it did not exceed 1% in all cases.

In real experiments, some assumptions of our theoretical model can be fulfilled only approximately. This concerns the shape of erythrocytes in a shear flow, their distribution in size and deformability, location and orientation in space, the assumption that there are no other light-scattering particles in the measuring volume, etc. If necessary, these circumstances can be taken into account in the theory, but this will lead to its significant complication. On the other hand, it is possible to bring the theory closer to the experiment by selecting the experimental conditions, such as the method of preparing blood samples, choosing the optimal shear stress and the coordinate system on the observation screen, etc. The final verification and assessment of the accuracy of the model can be carried out in experiments with specially prepared blood samples.

10 Conclusion

In this paper, we consider the problem of measuring the fraction of weakly deformable erythrocytes (FWDE) in a blood sample by laser diffractometry of erythrocytes in a shear flow (ektacytometry). The parameters of the diffraction pattern that are most sensitive to FWDE are revealed. These parameters are the coordinates of the polar and characteristic points of the isointensity line. An algorithm for measuring FWDE is proposed based on a comparison of experimentally observed diffraction patterns with patterns calculated in the bimodal ensemble approximation, when only two types of erythrocytes are present in a blood sample – normal (deformable) and rigid (non-deformable) erythrocytes. The accuracy of the algorithm was estimated by numerical experiment and the area of its applicability was determined both in relation to the allowable inhomogeneity of the ensemble of erythrocytes and in relation to the part of the diffraction pattern suitable for measurements. The calculations are made for typical experimental conditions, when the aspect ratio of the isointensity line chosen for measurements is $D = 2 \div 3$. It is shown that the measurement error of FWDE does not exceed 10% if the spread of erythrocytes in deformability is $\mu' = 6 \div 23$ %, and the light intensity on the isointensity line is $\tilde{I} = 3 \div 9$ % relative to the intensity of the central maximum of the diffraction pattern. For light intensity levels $\tilde{I} = 25 \div 40$ %, the measurement error of FWDE, as a rule, exceeds 10%. These data confirm the earlier conclusion that the most sensitive to the parameters of the ensemble of erythrocytes is that part of the diffraction pattern, where the light intensity is approximately an order of magnitude lower than the intensity of the central

diffraction maximum. The aspect ratio for the soft component of the ensemble of erythrocytes (parameter s_2) in all cases considered by us was found with an error not exceeding 1%.

Acknowledgments

This work was supported by the Russian Science Foundation (grants 18-71-00158 and 22-15-00120) and by the Ministry of Education and Science of the Russian Federation as part of the program of the Moscow Center for Fundamental and Applied Mathematics under the agreement № 075-15-2022-284 as well as by Interdisciplinary Scientific and Educational School of Moscow University "Photonic and Quantum Technologies. Digital Medicine".

Disclosures

The authors declare no conflict of interest.

References

1. E. Ch. Mokken, M. Kedaria, Ch. P. Henny, M. R. Hardeman, and A. W. Gelb, "The clinical importance of erythrocyte deformability, a hemorrheological parameter," Annals of Hematology 64, 113–122 (1992).
2. S. Shin, Y. Ku, M. S. Park, and J. S. Suh, "Deformability of red blood cells: A determinant of blood viscosity," Journal of Mechanical Science and Technology 19, 216–223 (2005).
3. O. K. Baskurt, M. Boynard, G. C. Cokelet, P. Connes, B. M. Cooke, S. Forconi, F. Liao, M. R. Hardeman, F. Jung, H. J. Meiselman, G. Nash, N. Nemeth, B. Neu, B. Sandhagen, S. Shin, G. Thurston, and J. L. Wautier, "New guidelines for hemorheological laboratory techniques," Clinical Hemorheology and Microcirculation 42(2), 75–97 (2009).
4. T. J. McMahon, "Red BloodCell Deformability, Vasoactive Mediators, and Adhesion," Frontiers in Physiology 10, 1417 (2019).
5. M. Bessis, N. Mohandas, "A diffractometric method for the measurement of cellular deformability," Blood Cells 1, 307–313 (1975).
6. N. Nemeth, F. Kiss, and K. Miszti–Blasius, "Interpretation of osmotic gradient ektacytometry (osmoscan) data: A comparative study for methodological standards," Scandinavian Journal of Clinical and Laboratory Investigation 75(3), 213–222 (2015).
7. A. Sadaf, K. G. Seu, E. Thaman, R. Fessler, D. G. Konstantinidis, H. A. Bonar, J. Korpik, R. E. Ware, P. T. McGann, C. T. Quinn, and T. A. Kalfa, "Automated Oxygen Gradient Ektacytometry: A Novel Biomarker in Sickle Cell Anemia," Frontiers in Physiology 12, 636609 (2021).
8. A. U. Zaidi, S. Buck, M. Gadgeel, M. Herrera–Martinez, A. Mohan, K. Johnson, S. Bagla, R. M. Johnson, and Y. Ravindranath, "Clinical Diagnosis of Red Cell Membrane Disorders: Comparison of Osmotic Gradient Ektacytometry and Eosin Maleimide (EMA) Fluorescence Test for Red Cell Band 3 (AE1, SLC4A1) Content for Clinical Diagnosis," Frontiers in Physiology 11, 636 (2020).
9. M. A. E. Rab, B. A. van Oirschot, J. Bos, T. H. Merkx, A. C. W. van Wesel, O. Abdulmalik, M. K. Safo, B. A. Versluijs, M. E. Houwing, M. H. Cnossen, J. Riedl, R. E. G. Schutgens, G. Pasterkamp, M. Bartels, E. J. van Beers, and R. van Wijk, "Rapid and reproducible characterization of sickling during automated deoxygenation in sickle cell disease patients," American Journal of Hematology 94(5), 575–584 (2019).
10. O. K. Baskurt, M. R. Hardeman, M. Uyuklu, P. Ulker, M. Cengiz, N. Nemeth, S. Shin, T. Alexy, and H. J. Meiselman, "Comparison of three commercially available ektacytometers with different shearing geometries," Biorheology 46(3), 251–264 (2009).
11. J. G. G. Dobbe, M. R. Hardeman, G. J. Streekstra, J. Starckee, C. Ince, and C. A. Grimbergen, "Analyzing red blood cell–deformability distributions," Blood Cells, Molecules, and Diseases 28(3), 373–384 (2002).
12. J. G. G. Dobbe, G. J. Streekstra, M. R. Hardeman, C. Ince, and C. A. Grimbergen, "Measurement of the Distribution of Red Blood Cell Deformability Using an Automated Rheoscope," Cytometry: The Journal of the International Society for Analytical Cytology 50(6), 313–325 (2002).
13. S. Yu. Nikitin, A. E. Lugovtsov, V. D. Ustinov, M. D. Lin, and A. V. Priezzhev, "Study of laser beam scattering by inhomogeneous ensemble of red blood cells in a shear flow," Journal of Innovative Optical Health Science 8(4), 1550031 (2015).
14. N. L. Parrow, P.-C. Violet, H. Tu, J. Nichols, C. A. Pittman, C. Fitzhugh, R. E. Fleming, N. Mohandas, J. F. Tisdale, and M. Levine, "Measuring Deformability and Red Cell Heterogeneity in Blood by Ektacytometry," Journal of Visualized Experiments (131), e56910 (2018).
15. J. Plasek, T. Marik, "Determination of undeformable erythrocytes in blood samples using laser light scattering," Applied Optics 21(23), 4335–4338 (1982).
16. G. J. Streekstra, J. G. G. Dobbe, and A. G. Hoekstra, "Quantification of the poorly deformable red blood cells using ektacytometry," Optics Express 18(13), 14173–14182 (2010).
17. Y. Man, R. An, K. Monchamp, Z. Sekyonda, E. Kucukal, C. Federici, W. J. Wulftange, U. Goreke, A. Bode, V. A. Sheehan, and U. A. Gurkan, "Occlusion Chip: A functional microcapillary occlusion assay complementary to

ektacytometry for detection of small–fraction red blood cells with abnormal deformability," Frontiers in Physiology 13, 954106 (2022).
18. Y. J. Kang, S. Serhrouchni, A. Makhro, A. Bogdanova, and S. S. Lee, "Simple Assessment of Red Blood Cell Deformability Using Blood Pressure in Capillary Channels for Effective Detection of Subpopulations in Red Blood Cells," American Chemical Society Omega 7(43), 38576–38588 (2022).
19. M. Grau, L. Kuck, T. Dietz, W. Bloch, and M. J. Simmonds, "Sub–Fractions of Red Blood Cells Respond Differently to Shear Exposure Following Superoxide Treatment," Biology 10(1), 47 (2021).
20. S. Yu. Nikitin, A. V. Priezzhev, and A. E. Lugovtsov, "Laser Diffraction by the Erythrocytes and Deformability Measurements," Chapter 6 in Advanced Optical Flow Cytometry: Methods and Disease Diagnoses, V. V. Tuchin (Ed.), 1st ed., John Wiley & Sons, 133–154 (2011). ISBN:9783527634286.
21. S. Yu. Nikitin, A.V. Priezzhev, and A. E. Lugovtsov, "Analysis of laser beam scattering by an ensemble of particles modeling red blood cells in ektacytometer," Journal of Quantitative Spectroscopy and Radiative Transfer 121, 1–8 (2013).
22. S. Yu. Nikitin, V. D. Ustinov, S. D. Shishkin, and M. S. Lebedeva, "Line curvature algorithm in laser ektacytometry of red blood cells," Quantum Electronics 50(9), 888–894 (2020).
23. S. Yu. Nikitin, V. D. Ustinov, "Characteristic point algorithm in laser ektacytometry of red blood cells," Quantum Electronics 48(1), 70–74 (2018).
24. S. Yu. Nikitin, V. D. Ustinov, and S. D. Shishkin, "Band point algorithms for measuring diffraction pattern parameters in laser ektacytometry of red blood cells," Quantum Electronics 51(4), 353–358 (2021).